

# Thick Disks of Lenticular Galaxies <sup>★</sup>

## 3D-photometric thin/thick disk decomposition of eight edge-on S0 galaxies

M. Pohlen<sup>1,2</sup>, M. Balcells<sup>1</sup>, R. Lütticke<sup>3,2</sup>, and R.-J. Dettmar<sup>2</sup>

<sup>1</sup> Instituto de Astrofísica de Canarias, E-38200 La Laguna, Tenerife, Spain  
e-mail: [pohlen,balcells@ll.iac.es](mailto:pohlen,balcells@ll.iac.es)

<sup>2</sup> Astronomical Institute, Ruhr-Universität Bochum, D-44780 Bochum, Germany  
e-mail: [dettmar@astro.rub.de](mailto:dettmar@astro.rub.de)

<sup>3</sup> Department of Computer Science, FernUniversität Hagen, D-58084 Hagen, Germany  
e-mail: [Rainer.Luetticke@FernUni-Hagen.de](mailto:Rainer.Luetticke@FernUni-Hagen.de)

Received 23 December, 2003; accepted 04 March, 2004

**Abstract.** Thick disks are faint and extended stellar components found around several disk galaxies including our Milky Way. The Milky Way thick disk, the only one studied in detail, contains mostly old disk stars ( $\approx 10$  Gyr), so that thick disks are likely to trace the early stages of disk evolution. Previous detections of thick disk stellar light in external galaxies have been originally made for early-type, edge-on galaxies but detailed 2D thick/thin disk decompositions have been reported for only a scant handful of mostly late-type disk galaxies. We present in this paper for the first time explicit 3D thick/thin disk decompositions characterising the presence and properties (e.g. scalelength and scaleheight) for a sample of eight lenticular galaxies by fitting 3D disk models to the data. For six out of the eight galaxies we were able to derive a consistent thin/thick disk model. The mean scaleheight of the thick disk is 3.6 times larger than that of the thin disk. The scalelength of the thick disk is about twice, and its central luminosity density between 3-10% of, the thin disk value. Both thin and thick disk are truncated at similar radii. This implies that thick disks extend over fewer scalelengths than thin disks, and turning a thin disk into a thick one requires therefore vertical but little radial heating. All these structural parameters are similar to thick disk parameters for later Hubble-type galaxies previously studied. We discuss our data in respect to present models for the origin of thick disks, either as pre- or post-thin-disk structures, providing new observational constraints.

**Key words.** Galaxies: photometry – Galaxies: bulges – Galaxies: structure – Galaxies: fundamental parameters – Galaxies: evolution – Galaxies: formation – Galaxies: individual: ESO311-012, NGC1596, NGC2310, NGC3564, NGC3957, NGC4179, NGC4521, NGC5047

### 1. Introduction

The knowledge of the detailed distribution of stars in galaxies is of fundamental importance to address the formation and evolution of those systems. To a first approximation, a disk galaxy can be described by a set of distinct stellar entities: a disk population, a bulge component, and a stellar halo. Deep surface photometry of external early-type galaxies (Burstein, 1979a,b,c; Tsikoudi, 1979, 1980) and later elaborate measurements in our own Galaxy (Gilmore & Reid, 1983) revealed the need for an additional component of stars. This was called ‘thick disk’ (Burstein, 1979c), since it exhibiting a disk-like distribu-

tion with larger scaleheight compared to the inner, dominating ‘thin disk’.

There are three distinct families of hypotheses for its creation. The first group considers the thick disk as a separate entity produced in an early phase of enhanced star formation during the initial proto-galactic collapse (i.e. the ELS scenario, Eggen, Lynden-Bell, & Sandage, 1962; Gilmore, 1984; Burkert, Truran, & Hensler, 1992). Another family of models regards the thick disk as an extension (by dynamical heating) of the thin disk. They assume that after the initial collapse all gas settles down into the galactic plane and starts forming stars. On this thin stellar disk a variety of constant or violent heating mechanisms could act: spiral density waves (Barbanis & Woltjer, 1967; Carlberg & Sellwood, 1985), encounters with giant molecular clouds (e.g. Spitzer & Schwarzschild, 1953; Lacey, 1984), scattering by

Send offprint requests to: M. Pohlen

<sup>★</sup> Based on observations obtained at the European Southern Observatory, Chile

Galaxy	RA	DEC	RC3	T	Diam.	$v_{\odot}$	$v_{\text{vir}}$	D	$M_{\text{B}}^0$
	(2000.0)		type		[ ' ]	[ km s <sup>-1</sup> ]	[ km s <sup>-1</sup> ]	[ Mpc ]	[ mag ]
(1)	(2)	(3)	(4)	(5)	(6)	(7)	(8)	(9)	(10)
NGC 1596	04 27 38.1	-55 01 40	.LA..*/	-2.0	3.9	1510	1229	17.1	-19.3
NGC 2310	06 53 54.0	-40 51 45	.L....	-2.0	4.1	1187	943	13.1	-18.6
ESO 311-012	07 47 34.1	-41 27 08	.S..0?/	0.0	3.7	1131	893	12.4	-20.0
NGC 3564	11 10 36.4	-37 32 51	.L...*/	-2.0	1.7	2812	2639	36.7	-20.2
NGC 3957	11 54 01.5	-19 34 08	.LA.+*/	-1.0	3.1	1687	1607	22.3	-19.0
NGC 4179	12 12 52.6	+01 17 47	.L....	-2.0	4.1	1248	1277	17.7	-19.6
NGC 4521	12 32 47.7	+63 56 21	.S..0..	0.0	2.6	2500	2767	38.4	-20.2
NGC 5047	13 15 48.5	-16 31 08	.L....	-2.0	2.7	6330	6292	87.4	-21.7

**Table 1.** Global parameters of the observed lenticular galaxies: (1) Principal name, (2) right ascension, (3) declination, (4) RC3 coded Hubble-type, and the (5) Hubble parameter T are taken from de Vaucouleurs et al. (1991). The (6) diameter in arcminutes, the (7) heliocentric radial velocities, and the B-Band absolute magnitude (10) are taken from LEDA. According to the heliocentric radial velocities corrected for the Local Group infall into the Virgo cluster (8) from LEDA, we estimated the (9) distances following the Hubble relation with the Hubble constant from the HST key project of  $H_0 = 72 \text{ km s}^{-1} \text{ Mpc}^{-1}$  (Freedman et al., 2001).

massive black holes (Lacey & Ostriker, 1985), energy input by accretion of satellite galaxies (Carney et al., 1989; Quinn, Hernquist, & Fullagar, 1993; Velazquez & White, 1999; Aguerri et al., 2001), or bar bending instabilities (Raha et al., 1991). For example, Gnedin (2003) recently used N-body simulations to show that tidal heating in a cluster is sufficient to thicken stellar disks by a factor of 2-3. This kinematic heating and vertical expansion will lead to a significant morphological transformation of a normal spiral galaxy into a lenticular. The third model suggests that thick disks are mostly made of debris material from accreted satellites. Recent cosmological N-body+SPH galaxy formation models of Abadi et al. (2003) locating the thick disk formation before  $z \approx 1$  find that more than half of the thick disk stars are actually tidal debris from disrupted satellites. Therefore the thick disk is not a former thin disk thickened by a minor merger. To decide which of these hypotheses could explain the thick disk phenomenon best we need first a more general and complete statistic of thick disk properties. Naturally, these are rather global ones for external galaxies whereas our particular position in the Milky Way makes it possible to determine much finer details.

Since the work of Tsikoudi and Burstein (Burstein, 1979a,b,c; Tsikoudi, 1979, 1980) it appears well known that thick disks are quite common in S0 galaxies. However, none of the more recent detections, except for two galaxies in de Grijs & van der Kruit (1996) and a short remark in de Grijs & Peletier (1997), quantifying detailed parameters such as the ratio of thick to thin disk scaleheight or scalelength, is actually made in S0 galaxies. All these galaxies are of later Hubble type. In addition, we have not found a detailed 2D thin/thick disk decomposition for any S0 galaxy in the literature. Subsequent numerical decompositions dealing with S0 galaxies after the pioneering work in the

early 80's treated the thick disk either as an outer flattened but exponential halo (for NGC 4452 and NGC 4762: Hamabe & Wakamatsu, 1989), or as a spheroidal bulge component (for NGC 1381: de Carvalho & da Costa, 1987) (for NGC 3115: Capaccioli, Held, & Nieto, 1987; Silva et al., 1989).

The detections of possible halo or thick disk stellar light in disk galaxies of later Hubble type have been made in a scant handful of mostly nearby edge-on galaxies (e.g. for ESO 342-017, IC 5249, NGC 891, NGC 4565, NGC 5907, and NGC 6504: van der Kruit & Searle, 1981a,b; Shaw & Gilmore, 1989; Morrison, Boroson, & Harding, 1994; van Dokkum et al., 1994; Sackett et al., 1994; Morrison et al., 1997; Näslund & Jörsäter, 1997; Lequeux et al., 1998; Zheng et al., 1999; Neeser et al., 2002). Quite recently, Dalcanton & Bernstein (2002) suggest the detection of extended, ubiquitous thick disks in a large sample of late-type, edge-on galaxies by means of multi-colour imaging. However, their thick disks are solely detected by vertical colour gradients for which dust extinction complicates the interpretation. In addition, their vertical colour profiles, especially  $(R - K)$ , typically extend out to only very few vertical disk scaleheights. At those z-heights where they attribute the red colour to an additional component the thin disk may still be dominant over a potential thick disk and even determine the measured colour.

In this paper, we analyse a set of eight edge-on S0 galaxies using the classical approach for the identification of thick disks in external galaxies: the need for an additional disk component when attempting to fit single disk models to the light distribution in a deep image. Thereby we characterise the presence and properties (scalelengths, -heights, and central surface brightnesses) of thick disks by directly measuring their structure.

## 2. Sample Selection & Observations

The data were taken as part of the PhD study on the radial structure on galactic stellar disks by Pohlen (2001). The galaxies were selected according to the allocated observing time, observatory, and CCD-chip size meeting the following morphological selection criteria. Using images from the Digitized Sky Survey (DSS) we verified that they are edge-on ( $i \gtrsim 86^\circ$ ), undisturbed, and similar to some disk-prototypical cases like NGC 4565 or IC 2531 to make it possible to consistently fit the applied simple disk model (cf. Sect. 3). Galaxies with the following characteristics were rejected: spiral arms (indicating towards a lower inclination), a significantly asymmetric or disturbed disk (indicating towards strong interaction), and two-sided or significantly one-sided warped disks. In addition, galaxies which seemed to be dominated by the light of the bulge component, or appeared to be too small ( $D_{25} \gtrsim 2''$ ), or showed only a faint, patchy disk were also excluded. For the observed lenticulars we therefore selected galaxies with a symmetric, smooth disk and a distinct, non-dominant bulge component. It is not unexpected that half of these galaxies show a box- or peanut-shaped (b/p) bulge component, since Lütticke et al. (2000a) find that  $> 40\%$  of all bulges are b/p shaped. Global properties of the finally observed eight S0 galaxies are given in Table 1. We do not argue that this sample is fully representative of the general population of S0 galaxies but it ensures the best prospects for obtaining consistent models with our 3D modelling technique for all galaxies.

The images (in Johnson R or V filter) were obtained in four observing runs in 1998/1999, three at the Danish 1.54m telescope of the European Southern Observatory (ESO, Chile) and one at the 1.23m telescope on Calar Alto (CAHA, Spain). During all three runs at the ESO the 1.54m Danish telescope was equipped with DFOSC and the C1W7/CCD which is a 2k x 2k LORAL chip providing a field size of  $\approx 13'$  and a scale of  $\approx 0.39''$  pixel $^{-1}$ . The run at the Calar Alto 1.23m telescope was done in service mode with the Site#18b chip, a 2048x2048 SITE CCD with 24  $\mu$ m pixel size, providing an unvignetted field of  $\approx 10'$  and a scale of  $\approx 0.5''$  pixel $^{-1}$ .

The standard CCD reduction techniques —overscan correction; subtraction of remaining large scale gradient in combined, overscan-subtracted, masterbias image; and careful flatfielding— were applied using the IRAF data reduction package. Neither the DFOSC nor the Calar Alto CCD R-band images were affected by fringing. The individual, dithered, reduced short exposures (150 s–600 s) were combined to the final deep image using IRAF's *imcombine* task. These images are rotated to the major axis using the smallest angle of rotation according to their true position on the sky. Table 2 summarises the detailed observational parameters. During the two ESO observing runs in 1999 several Landolt (1992) fields, partly enriched with additional stars provided by B. Skiff (priv. comm.), were observed. The standard fields were taken at least three times a night at different airmasses to determine the at-

mospheric extinction. During the other two observing runs no standard stars were taken. The ESO run in 1998 is calibrated by literature values and for galaxies without catalogued values interpolated according to the measured sky background. Only a rough zero point could be estimated for the Calar Alto run by comparing a galaxy also observed in another calibrated Calar Alto run. For more details about the photometric calibration we refer to Pohlen (2001).

## 3. Extraction of the Disk Parameters

### 3.1. 3-Dimensional Disk Model

We have developed a semi-automatic recipe to fit true 3-D single-component luminosity distributions to the 2-D data of edge-on galaxies and determine the galaxy parameters, such as scalelength and scaleheight in a physically meaningful way. Our method is described in detail in Pohlen et al. (2000b) and Pohlen (2001) and is only briefly recalled here. The disk model is based upon the fundamental work of van der Kruit & Searle (1981a). They tried to find a fitting function for the three-dimensional light distribution in disks of edge-on galaxies using the empirically determined exponential radial gradient,  $I \propto \exp(R)$ , and adding a description for the vertical distribution,  $f(z)$ , of the stars. The luminosity density distribution  $\hat{L}(R, z)$  can be written as:

$$\hat{L}(R, z) = \hat{L}_0 \exp\left(-\frac{R}{h}\right) f_n(z, z_0) H(R_{\text{co}} - R) \quad (1)$$

$\hat{L}$  being the luminosity density in units of [ $L_\odot$  pc $^{-3}$ ],  $\hat{L}_0$  the central luminosity density,  $R$  and  $z$  are the radial resp. vertical axes in cylinder coordinates,  $h$  is the radial scalelength and  $z_0$  the scaleheight, and  $n$  the index of the vertical distribution function.  $H(x_0 - x)$  is the Heaviside function and  $R_{\text{co}}$  is the cut-off radius characterising the observed outer radial truncations (van der Kruit, 1979; Pohlen et al., 2002, and references therein). To limit the choice of parameters we restrict our models to the three main density laws for the  $z$ -distribution (exp, sech, and sech $^2$ ) following van der Kruit (1988). Due to the choice of our normalised isothermal case  $z_0$  is equal to  $2h_z$ , where  $h_z$  is the usual exponential vertical scale height preferred by many authors:

$$f_1(z) = 4 \exp\left(-2 \frac{|z|}{z_0}\right)$$

$$f_2(z) = 2 \operatorname{sech}\left(\frac{2z}{z_0}\right)$$

$$f_3(z) = \operatorname{sech}^2\left(\frac{z}{z_0}\right)$$

For any details about the numerical realisation we refer to Pohlen et al. (2000b). Therefore six free parameters ( $i$ ,  $n$ ,  $\hat{L}_0$ ,  $R_{\text{co}}$ ,  $h$ ,  $z_0$ ) fit the observed surface intensity on the CCD chip to the model. This model assumes that the vertical distribution is independent of position along the

Galaxy	Filter	Date [mmyy]	Site	Exp.time [min]	Seeing ["]	Coadds # x [s]
(1)	(2)	(3)	(4)	(5)	(6)	(7)
NGC 1596	R	0198	ESO	45.0	1.3	8x300, 2x150
NGC 2310	R	0198	ESO	51.7	1.3	600, 500, 200, 9x200
ESO 311-012	V	0599	ESO	60.0	1.6	12x300
NGC 3564	V	0399	ESO	66.3	1.3	600, 500, 3x360, 6x300
NGC 3957	R	0198	ESO	30.0	1.3	3x600
NGC 4179	V	0599	ESO	65.0	1.6	1x600, 1x480, 1x360, 1x300, 9x240
NGC 4521	R	0699	CAHA	60.0	1.5	6x600
NGC 5047	V	0599	ESO	60.0	1.5	6x600

**Table 2.** Observing log for the individual combined images with (1) the galaxy, (2) the filter, (3) the observing date, (4) the site, (5) the total coadded on-source exposure time  $t_{\text{int}}$ , (6) mean seeing conditions during the observations, (7) the number of individual images with their  $t_{\text{int}}$ .

major axis as is known to be true in good approximation (cf. e.g. van der Kruit & Searle, 1981a; Shaw & Gilmore, 1990). The increase of scaleheight with galactocentric distance as reported by de Grijs & Peletier (1997) can be described as a combination of two disks each with constant scaleheight but different scalelength (cf. Sect. 3.2). Any deviation from constant scaleheights should be visible in the vertical profiles overplotted by the models, which is not the case (cf. Appendix B). The apparent small vertical shift of some models in the lowest plotted vertical profile is due to the change in radial scalelength, as described in Sect. 3.4.

The possible influence on the six free parameters of the dust distribution, which was neglected during the fit, is estimated in Pohlen et al. (2000b). There we have shown that even for a worst case scenario (large optical depth  $\tau_R$  and a radially and vertically fairly extended dust lane) our model is able to reproduce the input parameters with an error of a typical 20%. We expect this effect to be even less significant for the present sample of lenticular, dust-depleted galaxies. Deriving individual errors on all parameters is a complex task since the main source of error is not the numerical fitting procedure ( $< 1\%$ ) but the systematic uncertainties in the process of fitting a rather simple, empirical model to real galaxies. An estimation of the errors is given in Pohlen et al. (2000b) by changing the applied boundaries of the region used to fit the data to the model (cf. also Pohlen, 2001). They found differences in  $h$  and  $z_0$  of about 15% and  $\hat{L}_0$  varied about a factor of two. This is in the same range found by Knapen & van der Kruit (1991) when they compared published values of scalelength measurements from different studies.

### 3.2. Thin/thick disks

Pohlen (2001) noted that the S0 galaxies in his sample are not well described by any combination of a single disk and another spheroidal component, such as a de Vaucouleurs  $R^{1/4}$  bulge model (de Vaucouleurs, 1948). All S0 galaxies

reveal a typical, continuous change of slope when one compares the major axis with parallel profiles above/below the plane. The profiles significantly flatten towards cuts higher above the midplane. According to the single component model  $\hat{L}(R, z)$  all slopes should be nearly parallel. We infer from the images (cf. Appendix B) that all S0 galaxies show a kind of smooth outer envelope or highly flattened spheroidal component. This deviation from a normal shape cannot be explained by a bulge component. Any large  $R^{1/4}$  bulge would have to be apparent on the major axis which is certainly dominated by an exponential (disk) component. It is worth mentioning that in the sample of Pohlen (2001) there are four galaxies, NGC 3390 ( $T=3$ ), NGC 3717 ( $T=3$ ), NGC 4696C ( $T=3.4$ ), and NGC 6504 ( $T=2$ )<sup>a</sup> that showed a similar behaviour but were classified as late-type galaxies.

The outer component could be described as a ‘thick disk’ according to Burstein (1979c) with a flatter slope than the inner thin disk, equivalent to a larger scalelength. However, the main characteristic of a thick disk is that the observed vertical profiles depart from the simple exponential model. Compared to the model, the outer parts are systematically brighter with increasing distance to the major axis. As mentioned by de Grijs & Peletier (1997), the measured increase of the scaleheight with radius (‘flaring’) for early-type, edge-on disk galaxies can be understood if these galaxies have both thick disk scalelengths and scaleheights larger than for the dominant old disk.

### 3.3. Fitting Method

To apply our single component fitting method described in the previous section we have to assume that there is a region in the galaxy dominated by only one of the components. If one uses exponential profiles it is obvious from the vertical and radial cuts that there are well separated

<sup>a</sup> The classification is done by Lütticke et al. (2000a). It is consistent with that of van Dokkum et al. (1994), but significantly different from that of the UGC catalogue (Nilson, 1973).

vertical ranges (around the major axis and the outermost profiles) in which the light of one of the two disks dominates. Fitting thin and thick disk component simultaneously would be the desired approach. However, our single component model has already six free parameters. As shown in Pohlen (2001), fitting this model to observed data is a non-trivial task. The problem is the application of an idealized model itself, which obviously will not totally accurately describe the measured two-dimensional light distribution. This technique requires continuous human supervision to control the influence and quality of each individual parameter. This would most probably be even more difficult for a parameter set twice as large. We decided therefore to use an iterative fitting routine starting from outside-in since the thick disk clearly dominates the outer parts. The first step is to determine an initial estimate for the outer disk by restricting the region to be fitted and using our single component model. The next step is subtracting the derived full thick disk model from the original image and fit an inner disk to the residual by restricting the fitting range to the inner parts. Then we start from the beginning by subtracting this inner disk model from the original image and fit again the outer disk, now to this residual image. The initially pre-defined fitting regions for the thin and thick disk are sometimes adapted slightly after subtracting one of the components and before starting the second fitting round. As it turned out this process is remarkably stable for most of the galaxies. After one iteration the disk parameters are already the same within the range of one single model. The reason for this is the domination of the thick disk at large vertical  $z$ -heights ( $\gtrsim 3.5z_0^n = 7h_z^n$ ) measured here with high S/N, and the large radial range used to fit the thick disk component.

To restrict the number of free parameters we decided to prefix the inclination during the fitting process for this sample. For most of the galaxies the symmetric shape of the bulge and disk component indicates an exactly edge-on orientation. Only one of the S0 galaxies (NGC 3957) exhibits a dust-lane making it possible to estimate the inclination at  $i = 88^\circ \pm 1^\circ$  following the method by Barteldrees & Dettmar (1994).

The different density laws for the vertical distribution are similar for large  $z$  and only differ around the mid-plane of the luminosity distribution (cf. Fig. 4 in de Grijs, Peletier, & van der Kruit, 1997). In Pohlen et al. (2000b) the actual choice of one fitting function is done individually for each galaxy depending on the measured profiles. However, near the plane of the galaxy the contribution of a thick disk is much smaller than that of the thin disk component. First tests with a free choice of the fitting function for the vertical density distribution (exp, sech, or  $\text{sech}^2$ ) showed in the case of ESO 311-012 that the iterative fit became unstable for this reason. In the subsequent modelling we have chosen the intermediate fitting function  $f_2(z) \propto \text{sech}(2z/z_0)$  in all cases for the thin and thick disk component. There was only one galaxy, NGC 2310, for which the sech function

did not yield a satisfying convergency of the iterative fitting. However, switching to  $\text{sech}^2$  significantly improved the fit. Finally, only three free parameters are left for each disk ( $\tilde{L}_0$ ,  $h$ ,  $z_0$ ).

We want to point out that these decompositions are thus model dependent. An isothermal thick disk contributes less light to the thin/thick disk combination than to an exponential one and the shape of the thin disk will also be different. In addition, vertical scaleheights  $z_0$  obtained with an exp model are systematically larger than in a sech model and again larger than in a  $\text{sech}^2$  fit. Depending on the vertical boundaries chosen for the fitting these differences could be more than 30%. The choice for the vertical distribution influences also the best-fit scale parameter ratio  $z_0^k/z_0^n$ . Shaw & Gilmore (1989) used all combinations of either  $\text{sech}^2$  or exp models for NGC 4565 and derived  $z_0^k/z_0^n$  in the range of 4.3 – 5.4.

In contrast with some of the previous 1-D-only fitting methods we do not simply use the deviation from a simple exponential on the minor axis, or parallel profiles; to measure thick disks we use the full 2-dimensional information and are therefore able to fit the radial scalelength of the thick disks.

### 3.4. Breaks in Radial Profiles

One of the main difficulties while properly fitting our model to the S0 galaxies is their outer disk structure. This will be discussed in detail in Pohlen et al. (2004) and only briefly addressed here. As one can see from the figures in Appendix B there are clear breaks in the outer parts of the radial profiles. These are similar to the truncations in more later-type galaxies (cf. Pohlen et al., 2002; Kregel, van der Kruit, & de Grijs, 2002; de Grijs, Kregel, & Wesson, 2001; Pohlen, Dettmar, & Lütticke, 2000a). For all galaxies (except ESO 311-012) a similar break, slightly less pronounced, is also seen in other radial cuts parallel to the major axis. Our model, according to Eq. (1), however, describes only an infinitely sharp truncation  $R_{\text{co}}$ . As shown in Pohlen (2001) this implies a tight coupling between the radial scalelength  $h$  and the cut-off radius  $R_{\text{co}}$ , when using our model fitting data with the observed breaks in the profiles. In addition, the sharply truncated model exhibits an intrinsic bending of the profile towards the outer parts (cf. Pohlen, 2001). This complicates the visual quality control compared to the more flat infinite exponential model without any truncation. Therefore we decided to use the infinite exponential model, realised within the same fitting program by fixing  $R_{\text{co}}$  to ten times the radial scalelength. For our thick/thin fitting we restricted the fitting region to points inside the observed break radius. However, fitting an infinite exponential model to the intrinsic two-slope profiles is also affected by systematic errors (cf. Pohlen, 2001; Pohlen et al., 2004). Depending on the ratio of the inner, shallow slope ( $h_{\text{in}}$ ) up to the break, to the steeper, outer slope ( $h_{\text{out}}$ )

beyond the break radius the determined scalelength will be systematically too small. Assuming a mean ratio of  $h_{\text{in}}/h_{\text{out}} = 4.4 \pm 1.7$  from a large, edge-on sample by Pohlen (2001) makes it possible to quantify the expected offset. The best fitting scalelength  $h_{\text{in}}$  will be about 26% larger compared to the intrinsic radial scalelength (cf. Pohlen et al., 2004).

Although the exact value of the scalelength is thus model dependent, neither  $z_0$  nor  $\mu_0$  are influenced by this problem. The derived scaleheights are independent of the scalelength and therefore robust, but of course still depending on the chosen density law (exp, sech, or sech<sup>2</sup>) for the z-distribution.

## 4. Results

For six (75%) out of the eight S0 galaxies we were able to derive consistent thick/thin disk solutions (cf. Sect. 4.1). The resulting best fit parameters are listed in Table 3 and Table 4 for the thick and thin disk, respectively. The resulting radial and vertical profiles overplotted by our best fitting model are shown in Appendix B. The derived thin disk scalelength and scaleheight values are consistent with those found in studies by Kregel, van der Kruit, & de Grijs (2002) and Pohlen (2001), containing mostly galaxies of Hubble type later than Sa.

The mean ratio of thick to thin scaleheight for the five galaxies with the same vertical model combinations (sech+sech) for the thick and thin disk is  $z_0^k/z_0^n = 3.6 \pm 1.0$  and for the scalelength  $h^k/h^n = 1.8 \pm 0.1$ . Including also NGC 2310 we find  $z_0^k/z_0^n = 3.4 \pm 1.0$  and  $h^k/h^n = 1.9 \pm 0.4$ . We derive central surface brightnesses (uncorrected for inclination) in the range of  $22.0 \lesssim \mu_0^k \lesssim 22.2$  R-mag/□'' and  $21.9 \lesssim \mu_0^k \lesssim 22.9$  V-mag/□'' for our thick disks compared to  $19.2 \lesssim \mu_0^n \lesssim 19.6$  R-mag/□'' and  $19.5 \lesssim \mu_0^n \lesssim 20.7$  V-mag/□'' for the thin disks. This implies that the contribution of the thick disk to the central surface brightness is about 10% of that of the thin disk. The thick disk central luminosity density  $\hat{L}_0^k$  ranges between 3.5% and about 10% (mean: 5.6%) of the thin disk value. The ratio of the total luminosities of the thick and thin disk is between about one third and one.

The profile on the minor axis in addition to radial cuts high above the major axis (cf. Appendix B) reveals that for four (NGC 2310, NGC 3564, NGC 4179, NGC 5047) out of the six fitted galaxies there is no significant bulge component visible at large vertical height above the disk. Even the apparently bulge dominated galaxy NGC 3564 is well described by a thick disk component. The remaining bulge light after subtraction of the thin/thick disk combination is comparable to that of the other galaxies. This implies that all bulges of our S0 galaxies could not be well described by a traditional de Vaucouleurs  $R^{1/4}$  bulge. In addition, any bulge component would be too flat to account for all the light high above the disk at large galactocentric radii.

Galaxy	vertical region $z$		radial region $R$	
	thin	thick	thin	thick
	["]		["]	
(1)	(2)		(3)	
NGC 2310	0-12	20-35	32-75	0-79
ESO 311-012	0-8	8-31	29-88	37-117
NGC 3564	0-4	22-32	20-32	0-52
NGC 3957	0-4	16-28	36-56	24-64
NGC 4179	0-12	31-55	43-69	0-88
NGC 5047	0-6	18-25	35-47	0-55

**Table 5.** Radial and vertical fitting regions for the thick/thin disk components with (1) galaxy name, (2) beginning and end of thick/thin disk vertical region, and (3) beginning and end of thick/thin disk radial region

### 4.1. Fitting regions

One of the important constraints for fitting empirical, surface photometric models to observed data is the definition of the actual regions which are marked to characterise the individual model components. Therefore we list in Table 5 for each galaxy the radial and vertical ranges where our thick/thin disk fit was applied. In all cases we restricted the two fitting regions to be distinct from each other and outside the dust lane (in the case of NGC 3957) or any bar/ring like feature visible in the radial profile. This is obvious for the first thick disk estimation. However, in principle one could extend the fitting range towards the inner/outer parts for the following thick/thin disk iterations, since the other component in each case has already been subtracted. In addition, we masked by hand bright stars and background galaxies, forcing the program to ignore these regions.

### 4.2. Comparison with Literature

Burstein (1979c) only describes the ‘thick disk’ component qualitatively as being more diffuse than that of the inner, dominating disk, and possessing a flattened shape. The important observation is that the scaleheight of a fitted exponential to the vertical profiles increases with radial distance  $R$ . He determines a flattening, defined as the intrinsic z-thickness compared to the diameter  $a$ , of  $z/a = 0.25 - 0.2$  at  $\mu_B = 25.0$  which is somewhere between thin disks ( $z/a \lesssim 0.1$ ) and E4 ellipticals ( $z/a = 0.6$ ) for five edge-on S0 galaxies. We find values of 0.29 (NGC 2310) or 0.32 (NGC 5047) comparing minor to major axis diameter at the second outermost contour (cf. Fig. B.2, B.8).

While comparing scale parameter ratios in the literature one has to keep in mind that they are often obtained with very different fitting methods and even different fitting functions for the vertical distribution of thin and thick disk light. As discussed in Sect. 3.3 this already implies systematic differences of at least 20%. Surprisingly, there are no detailed parameter studies for thick disks of S0 galaxies in the literature that provide

Galaxy	Dist.	Band	$\mu_0^k$	$z_0^k$			$h^k$			
				[ $''$ ]	[kpc]	[ $z_0^n$ ]	[ $''$ ]	[kpc]	[ $h^n$ ]	[ $z_0^k$ ]
(1)	(2)	(3)	(4)	(5)			(6)			
NGC 2310 <sup>a</sup>	13.1	R	22.0	19.8	1.3	2.4	62.8	4.0	2.6	3.2
E 311-012	12.4	V	22.3	18.8	1.1	2.6	41.5	2.5	1.9	2.2
NGC 3564	36.7	V	21.9	22.0	3.9	5.3	20.6	3.7	1.8	0.9
NGC 3957	22.3	R	22.2	20.8	2.3	3.4	33.9	3.7	1.6	1.6
NGC 4179	17.7	V	22.9	37.3	3.2	3.1	51.0	4.4	1.9	1.4
NGC 5047	87.4	V	22.9	19.7	8.3	3.4	39.4	16.7	1.7	2.0
mean						3.4			1.9	1.9

**Table 3.** Results for the thick disk: (1) Galaxy, (2) distance, (3) filter, (4) central surface brightness (uncorrected for inclination) of the thick disk model  $\mu_0^k$ , (5) vertical scaleheight  $z_0^k$  in arcsec, parsec, and in units of the thin disk vertical scaleheight  $z_0^n$ , and the (6) radial scalelength  $h^k$  in arcsec, kpc, in units of the thin disk radial scalelength  $h^n$ , and in units of the thick disk vertical scaleheight  $z_0^k$  <sup>a</sup> (used  $\text{sech}^2$  instead of  $\text{sech}$ )

Galaxy	Dist.	Band	$\mu_0^n$	$z_0^n$		$h^n$		
				[ $''$ ]	[kpc]	[ $''$ ]	[kpc]	[ $z_0^n$ ]
(1)	(2)	(3)	(4)	(5)		(6)		
NGC 2310	13.1	R	19.6	8.1	0.5	24.0	1.5	3.0
ESO 311-012	12.4	V	20.5	7.2	0.4	21.4	1.3	3.0
NGC 3564	36.7	V	19.5	4.2	0.7	11.3	2.0	2.7
NGC 3957	22.3	R	19.2	6.0	0.7	21.6	2.3	3.6
NGC 4179	17.7	V	20.2	12.1	1.0	26.2	2.3	2.2
NGC 5047	87.4	V	20.7	5.8	2.5	22.6	9.6	3.9
mean								3.1

**Table 4.** Results for the thin disk: (1) Galaxy, (2) distance, (3) filter, (4) central surface brightness (uncorrected for inclination) of the thin disk model  $\mu_0^n$ , (5) vertical scaleheight  $z_0^n$  in arcsec, and parsec, and the (6) radial scalelength  $h^n$  in arcsec, kpc, and in units of the thin disk vertical scaleheight  $z_0^n$

both scaleheight and scalelength ratios (cf. Sect. 1). The only scaleheight ratios for S0 galaxies (cf. Table 6) are given for two galaxies (NGC 4710, NGC 4762) in detail by de Grijs & van der Kruit (1996) and for five galaxies with Hubble type  $T \lesssim 0.0$  without providing the individual values or applied fitting functions by de Grijs & Peletier (1997). They find ratios of  $z_0^k/z_0^n = 1.8 - 4.6$ , which falls well within the range of values for our S0 galaxies.

There are clearly more studies in the literature that provide detailed parameters (scaleheights and often also scalelengths) for thick disks in galaxies of later morphological type.

Van Dokkum et al. (1994) modeled excess light at large vertical distance one-dimensionally with a thin/thick disk combination for the edge-on Sab galaxy NGC 6504. They found that the ratio of scaleheights is roughly 4, slightly higher than the mean value for our S0 sample. However, their central surface brightness for the thick disk is significantly lower ( $\Delta\mu_0 = 1.6 \text{ mag}$ ) than our value for NGC 3957. This effect is not related to the different fitting functions used since our  $\text{sech}$  model should tend to result in systematically lower values for  $\mu_0$  than in their exp model.

For the Milky Way, recent optical star-count measure-

ments by Larsen & Humphreys (2003) yield thin disk values of  $z_0^n = 300 \text{ pc}$  and  $h^n = 3.5 \text{ kpc}$ , and for the thick disk  $z_0^k = 900 \text{ pc}$  and  $h^k = 4.7 \text{ kpc}$ . These are similar to the infrared 2MASS star counts by Ojha (2001) with  $z_0^n = 260 \text{ pc}$ ,  $h^n = 2.8 \text{ kpc}$ ,  $z_0^k = 860 \text{ pc}$ , and  $h^k = 3.7 \text{ kpc}$ , keeping in mind that the near-infrared surveys always derive systematically smaller scalelengths than in the optical. The resulting ratio of thick to thin disk scaleheight is very similar to the mean value we find for our S0 galaxies but their ratio of the scalelengths is also smaller. Du et al. (2003) present a list of thick disk local normalizations (relative to the solar neighbourhood) obtained in different studies including their own measurements (cf. their Table 2). The quoted values range from 2% up to 13% with a mean value of about 6.1%, which agrees very well with the mean value of 5.6% for the central luminosity density of our S0 galaxies.

Morrison et al. (1997) used one-dimensional vertical fits to derive the thick and thin disk scaleheights of NGC 891, an edge-on Sb galaxy similar to our Milky Way. They quote a large range of possible  $z_0^k/z_0^n$  values which are consistent with our S0 disks. Previous modeling of NGC 891 by van der Kruit (1984) yield a ratio of  $z_0^k/z_0^n = 3.0$  for a three component (thin plus thick

Galaxy	Type	Model	$z_0^k/z_0^n$	$h^k/h^n$	$\mu_0^k$ [mag/□"] R V -band	$\mu_0^n$ [mag/□"] R V -band	Reference
(1)	(2)	(2)	(3)	(4)	(5)	(6)	(7)
5 galaxies <sup>a</sup>	S0	sech+sech	2.6 ↔ 5.3	1.7 ↔ 1.9	22.2 21.9↔22.9	19.2 19.5↔20.7	this study
NGC 4710	S0	sech+exp	3.2				DE96
NGC 4762	S0	sech+exp	4.6				DE96
5 galaxies	S0	—	1.8↔4.6				DE97
NGC 6504	Sab	exp + exp	4.0		23.8 —	18.2 —	VA94
NGC 891	Sb	exp + exp	2.3↔6.3				MO97
NGC 891 <sup>b</sup>	Sb	$R^{1/4}$ +sech <sup>2</sup> + exp	3.0				VA84
NGC 4565 <sup>c</sup>	Sb	sech <sup>2</sup> +sech <sup>2</sup> +halo	2.2	1.4			WU02
NGC 4565	Sb	sech <sup>2</sup> +sech <sup>2</sup>	4.6	1.4	23.7 —	19.6 —	SH89
NGC 4565	Sb	exp + exp	5.4	1.1	23.0 —	18.8 —	SH89
MW <sup>d</sup> (optical)	Sbc	exp + exp	3.0	1.3			LA03
MW <sup>d</sup> (NIR)	Sbc	exp + exp	3.3	1.3			OJ01
ESO 342-017	Scd	exp + exp	2.5	≥ 1.0	22.1 22.5	20.0 20.5	NE02
IC 5249	Sd	exp + exp	3.0	0.6			AB99

**Table 6.** Comparison with literature: (1) Galaxy name (2) morphological type, (3) ratio of thick to thin disk scale-height, (4) ratio of thick to thin disk scalelength, (5) central surface brightness of thick disk (if quoted), (6) central surface brightness of thin disk, (7) reference DE96:de Grijs & van der Kruit (1996), DE97:de Grijs & Peletier (1997), VA94:van Dokkum et al. (1994), WU02:Wu et al. (2002), MO97:Morrison et al. (1997), VA84:van der Kruit (1984), SH89:Shaw & Gilmore (1989), LA03:Larsen & Humphreys (2003), OJ01:Ojha (2001), NE02:Neeser et al. (2002), AB99:Abe et al. (1999)

<sup>a</sup> NGC 2310 excluded (only sech<sup>2</sup> model for thick disk) <sup>c</sup> three component model (thin disk, thick disk, and halo)

<sup>b</sup> three component model (bulge and thin plus thick disk) <sup>d</sup> starcount analysis

disk, and additional  $R^{1/4}$ -spheroid) fit which is also in the range of our S0 galaxies. The slightly higher value of the thick disk central luminosity density (17% of the thin disk) compared to our maximum of 10% could be explained by the additional contribution of the applied  $R^{1/4}$ -spheroid, especially high above/below the midplane. However, Bahcall & Kylafis (1985) already pointed out that in the case of NGC 891 a combination of thin plus thick disk and a model with only one disk and a  $R^{1/4}$ -spheroid both give a good description of the data used by van der Kruit (1984).

For another prominent edge-on Sb galaxy, NGC 4565, several attempts for a decomposition are available. More recently, Wu et al. (2002) presented a thin/thick plus halo decomposition from a deep intermediate-band (6660Å) image deriving values only slightly smaller than for our S0 galaxies (cf. Table 6). However, the two component disk models of NGC 4565 by Shaw & Gilmore (1989) yield significantly higher values for the ratio  $z_0^k/z_0^n$ . The light Wu et al. (2002) put down to a halo is here ascribed solely to a thick disk with a large scaleheight. There is a large variety of model combinations (with different components) possible (cf. Shaw & Gilmore, 1989; Näslund & Jörsäter, 1997), which complicates a direct comparison.

NGC 5907, another nearby edge-on Sc galaxy, is an even more complex case. It is not yet clear if the multiple detected extended light distribution

is a thick disk or a stellar halo component (cf. Morrison, Boroson, & Harding, 1994). Zheng et al. (1999) even concluded that NGC 5907 does not have a faint extended halo at all (but compare with discussion in Neeser et al. (2002) for this issue).

Abe et al. (1999) obtained a deep optical image of the edge-on Sd galaxy IC 5249. They detected additional light to that predicted by a single exponential disk and tried to fit a thick disk model. The scaleheight ratio of their best thick disk is well within the range for our S0 galaxies. However, the scalelength of the thick disk is exceptionally smaller compared to the thin disk and their central luminosity density ( $\hat{L}_0^n/\hat{L}_0^k = 7.4$ ) is noticeable larger than for our sample.

Recently, Neeser et al. (2002) reported for the first time the detection of a thick disk in a low surface brightness galaxy (ESO 342-017 classified as Scd). They find for the scaleheight a ratio of  $z_0^k/z_0^n = 2.5$  (close to our values for NGC 2310 and ESO 311-012) with a comparable or somewhat larger scalelength for the thick disk. The scaleheight ratio and unprojected central surface brightness (cf. Table 6) are surprisingly similar to the range of values found for our S0 galaxies.



## 5. Discussion

### 5.1. Thick disks: discrete or continuous?

A key question is: *How to describe a thick disk in general?* With reference to the proposed different formation scenarios described in Sect. 1 we can assume that the disk component is either characterised as a superposition of two discrete and independent isothermal disk systems (as done here), or built from the contribution of multiple velocity-dispersion components (e.g. Wielen et al., 1992; Dove & Thronson, 1993). These two approaches on how to treat a thick disk seem to be incompatible. Therefore any derived parameters for the two-disks model appear useless for the multi-component disk. In addition, the latter seems to be superior since it is consistent with the model of continuous disk heating leading to the well known observable age-velocity dispersion relation (Wielen, 1977).

However, Majewski (1993) already states in his review that detailed studies of the spatial and kinematical distribution of stars in the Milky Way do not make it possible to decide if the thick disk is a discrete component or a more continuous sequence of stellar populations. Recently, Nissen (2003) concluded that the latest studies (e.g. Bensby, Feltzing, & Lundström, 2003) argue for the separate entity picture. This confirms our result that 75% of the chosen S0 galaxies are well described with a distinct, two-component thin/thick disk system. Note that these results exclude all thick disk formation scenarios based solely on heating. Especially the elemental abundance trends found by Bensby, Feltzing, & Lundström (2003) favour a merger scenario where a satellite galaxy either merges with the parent galaxy or sheds significant amounts of its material to form the thick disk as proposed by Abadi et al. (2003).

However, as already noted by Jacobi & Kegel (1994) it does not seem possible to distinguish between our simple model and more sophisticated ones. Therefore the very good description with the applied discrete two-component system for our galaxies is only a first step towards studying the luminosity distribution of external galaxies. In addition, one has to keep in mind that our model only fits well in a restricted radial range (only out to  $2.2h^n - 3.9h^n$ ) where most of the inner part is “hidden” by the central bulge, bar, or ring components. One key to the nature of the thick disk may lie in studying the outer parts where the breaks in the radial profiles of both thin and thick disk should provide an additional constraint. Any vertical colour gradients could provide additional information but the only available colour map for our sample (NGC 3957 in Pohlen, 2001) suffers from low S/N and is not conclusive.

### 5.2. Are thick disks of S0s exceptional ?

The fact that the range of thick disk parameters for all known S0 galaxies are not too different from those of late-type galaxies, even compared to a low surface brightness Scd galaxy, is especially surprising, since at first glance

one expects S0 galaxies to possess more prominent thick disks. However, in terms of the thick-to-thin-disk scale-height ratio our values agree well with those derived for all other galaxies (cf. Table 6). Even taking into account the central surface brightness or central luminosity density the comparison yields similar values. Does this point to a general formation process for thick disks independent of bulge-to-disk ratio and Hubble type ? At this stage we are not able to answer this question. Although the numbers of galaxies used for the comparison are the same, all literature values come from different sources, using sometimes very different methods and models to derive their parameters. In the case of NGC 4565 it is obvious that depending on the model, one can find an even larger variety of  $z_0^k/z_0^n$ -values than the full range for our six galaxies. In addition, as pointed out by Knapen & van der Kruit (1991), and again discussed in detail by Pohlen (2001), fitting disk-model components to surface brightness data of edge-on galaxies is a delicate business, and comparing the results of different authors can be misleading. To overcome this problem one has to extend this survey of thick disk parameters also to late-type galaxies. To reduce the inevitable influence of their prominent dust lanes this has to be done in the near-infrared. After applying the same fitting method one is able to address the questions if thick disks are really common around all Hubble-types, and if their parameters are really similar, as suggested here. This would entail a common formation scenario for thick disks independent of their normal evolution along the Hubble sequence.

Of our galaxies with successful thick disk models there are only two for which there are rotational velocity measurements in the literature. Therefore any correlation between mass and thick disk parameters could not be derived. Consequently it is still unclear if the mass, as a galaxy characteristic, is related to the thick disk parameters.

### 5.3. Thick disk scalelengths

We find significantly larger scalelength ratios ( $h^k/h^n = 1.9$ ) for the thick disks of our S0 galaxies than in the literature ( $h^k/h^n \lesssim 1.4$ ). Is this a possible distinction in thick disk parameters between late-type and our early-type galaxies ? Again, differences in fitting methods, especially for the scalelength in edge-on galaxies, could be responsible for this apparent disagreement. In particular, fitting profiles with clear breaks using a single disk (with an infinitely sharp truncation or infinite exponential as done here) will entail systematic errors (cf. Sect. 3.4), therefore this question could only be addressed unambiguously applying exactly the same method to late-type galaxies.

However, although the exact number is uncertain the scalelength of the thick disk is without doubt systematically larger than that of the thin disk. Except in one case this is also true for all the literature values. Does this larger scalelength imply a different formation pro-

cess or even restrict the available formation scenarios ? At a first glance the different scalelengths contradict a dynamical heating scenario, since this should only alter the vertical distribution. However, assuming two distinct disk components with radially constant thickness the velocity dispersion scales with radius (van der Kruit & Freeman, 1986). It depends therefore on the exact way (radial distribution) the proposed mechanisms (cf. Sect. 1) dispense the energy in the vertical motions of the stars. In the case of heating the disk by satellite accretion, the N-body simulations of Quinn, Hernquist, & Fullagar (1993) show that the scalelength of the disk is nearly unchanged (even slightly smaller than the initial scalelength) for the inner parts (out to  $3h_{\text{ini}}$ ). Due to the migration of material outwards in radius, at larger radius (out to  $\approx 6h_{\text{ini}}$ ) the final disk shows a second shallower component (cf. their Fig. 4). However, Aguerri et al. (2001) find in their N-body simulation a global outward transport of disk material leading to a general increase of the disk scalelength of 10% to 60%. Although this increase is below our measured scalelength ratios, the latter seems to coincide in general with observations of larger thick disk scalelengths. One has to keep in mind that in the satellite accretion scenario a pre-existing thin disk gets heated. The thin disk to be observed today must be rebuilt out of gas remaining after the merger process. It is not guaranteed that this thin disk will have the same scalelength as its predecessor since we do not have a unique explanation of how the disk scalelength is determined out of an initial (or new) gas distribution (cf. Pohlen et al., 2000b).

Looking from a slightly different angle, one can also try to apply the larger thick disk scalelength as a general argument against an internal heating scenario. Assuming infinitely exponential disks, the larger scalelength implies a larger angular momentum content of the thick disk. Any valid heating mechanism must therefore add angular momentum, which is not the case for the internal heating scenarios. However, note that the disks are not at all infinitely exponential but show clear breaks in their profiles (cf. Sect. 3.4). The disks exhibit the break at roughly similar radial radius (e.g. Fig. B.8). In this sense the thick disk is truncated “earlier” (in respect to its scalelength) than the thin disk. In addition to a probably lower rotational velocity this could add up again to a similar angular momentum content for thick and thin disk, ruling out the whole argument against the heating scenarios. The key point here is again the origin of these breaks in the radial profiles.

#### 5.4. Residuals

In addition to comparing thick disks across a large range of characteristic parameters of galactic disks, fitting and subtracting a combined disk yields valuable information on the structure and size of galactic bulges. As discussed in Appendix A the residual images highlight the deviation of the galaxy from the disk model. Structures only

faintly indicated in the profiles become obvious. One important result related to this is that for our sample of S0 galaxies none of the present bulges could be described as a traditional early-type  $R^{1/4}$  bulge in agreement with Balcells et al. (2003). However, a detailed structural analysis of the remaining central structures has to be done with great care. As discussed in Sect. 3.3, choosing the vertical model is not a unique process and therefore any variation of  $f(z)$  for the thick and thin disk could alter the shape of the disk profile in the inner bulge parts. Especially for galaxies where the bulge component along the minor axis extends vertically above the disk (ESO 311-012 and NGC 3957) this could be even more unconstrained.

*Acknowledgements.* We thank Reynier Peletier for stimulating discussions and acknowledge useful suggestions by the referee, Richard de Grijs. Part of this work was supported by the German *Deutsche Forschungsgemeinschaft*, *DFG*. This research has made use the Lyon/Meudon Extragalactic Database (LEDa, <http://leda.univ-lyon1.fr>) and the NASA/IPAC Extragalactic Database (NED) which is operated by the Jet Propulsion Laboratory, California Institute of Technology, under contract with the National Aeronautics and Space Administration. It also uses the Digitized Sky Survey (DSS) based on photographic data obtained using Oschin Schmidt Telescope on Palomar Mountain and The UK Schmidt Telescope and produced at the Space Telescope Science Institute. This research has made use of NASA’s Astrophysics Data System Bibliographic Services.

#### References

- Abadi, M. G., Navarro, J. F., Steinmetz, M., Eke, V. R. 2003, *ApJ*, 597, 21
- Abe, F., Bond, I. A., Carter, B. et al. 1999, *AJ*, 118, 261
- Aguerrí, J. A. L., Balcells, M., & Peletier, R. F. 2001, *A&A*, 367, 428
- Bahcall, J. N. & Klyafis, N. D. 1985, *ApJ*, 288, 252
- Balcells, M., Graham, A. W., Domínguez-Palmero, L., & Peletier, R. F. 2003, *ApJ*, 582, L79
- Barbanis, B. & Woltjer, L. 1967, *ApJ*, 150, 461
- Barteldrees, A. & Dettmar, R.-J. 1994, *A&AS*, 103, 475
- Bensby, T., Feltzing, S., & Lundström, I. 2003, *A&A*, 410, 527
- Burkert, A., Truran, J. W., & Hensler, G. 1992, *ApJ*, 391, 651
- Burstein, D. 1979a, *ApJS*, 41, 435
- Burstein, D. 1979b, *ApJ*, 234, 435
- Burstein, D. 1979c, *ApJ*, 234, 829
- Capaccioli, M., Held, E. V., & Nieto, J. 1987, *AJ*, 94, 1519
- Carlberg R. G., Sellwood J. A., 1985, *ApJ*, 292, 79
- Carney B. W., Latham D. W., Laird J. B., 1989, *AJ*, 97, 423
- Dalcanton, J. J. & Bernstein, R. A. 2002, *AJ*, 124, 1328
- de Carvalho, R. R. & da Costa, L. N. 1987, *A&A*, 171, 66
- de Grijs, R., Kregel, M., & Wesson, K. H. 2001, *MNRAS*, 324, 1074
- de Grijs, R. & Peletier, R. F. 1997, *A&A*, 320, L21

- de Grijs, R., Peletier, R. F., & van der Kruit, P. C. 1997, *A&A*, 327, 966
- de Grijs, R. & van der Kruit, P. C. 1996, *A&AS*, 117, 19
- de Vaucouleurs, G. 1948, *Ann. d'Astrophys.*, 11, 247
- de Vaucouleurs, G., de Vaucouleurs, A., Corwin, H.G., Buta, R.J., Paturel, G., & Fouque, J.B. 1991, *Third reference catalogue of bright galaxies*, Springer-Verlag New York
- Dove, J. B. & Thronson, H. A. 1993, *ApJ*, 411, 632
- Du, C., Zhou, X, Ma, J. et al. 2003, *A&A*, 407, 541
- Eggen, O. J., Lynden-Bell, D., & Sandage, A. R. 1962, *ApJ*, 136, 748
- Freedman, W.L., Madore, B.F., Gibson, B.K. et al. 2001, *ApJ*, 553, 47
- Gilmore, G. & Reid, N. 1983, *MNRAS*, 202, 1025
- Gilmore, G. 1984, *MNRAS*, 207, 223
- Gnedin, O. Y. 2003, *ApJ*, 589, 752
- Hamabe, M. & Wakamatsu, K. 1989, *ApJ*, 339, 783
- Jacobi, S. & Kegel, W. H. 1994, *A&A*, 282, 401
- Knapen, J. H. & van der Kruit, P. C. 1991, *A&A*, 248, 57
- Kregel, M., van der Kruit, P. C., & de Grijs, R. 2002, *MNRAS*, 334, 646
- Lacey, C. G. 1984, *MNRAS*, 208, 687
- Lacey, C. G. & Ostriker, J. P. 1985, *ApJ*, 299, 633
- Landolt, A.U. 1992, *AJ*, 104, 340
- Larsen, J. A. & Humphreys, R. M. 2003, *AJ*, 125, 1958
- Lequeux, J., Combes, F., Dantel-Fort, M., Cuillandre, J.-C., Fort, B., & Mellier, Y. 1998, *A&A*, 334, L9
- Lütticke, R., Dettmar, R.-J., & Pohlen, M. 2000a, *A&AS*, 145, 405
- Lütticke, R., Dettmar, R.-J., & Pohlen, M. 2000b, *A&A*, 362, 435
- Majewski, S. R. 1993, *ARA&A*, 31, 575
- Morrison, H. L., Boroson, T. A., & Harding, P. 1994, *AJ*, 108, 1191
- Morrison, H. L., Miller, E. D., Harding, P., Stinebring, D. R., & Boroson, T. A. 1997, *AJ*, 113, 2061
- Näslund, M. & Jörsäter, S. 1997, *A&A*, 325, 915
- Neeser, M. J., Sackett, P. D., De Marchi, G., & Paresce, F. 2002, *A&A*, 383, 472
- Nilson P., 1973, *Uppsala General Catalogue of Galaxies*, Uppsala
- Nissen, P. E. 2003, *astro-ph/0310326*, *Carnegie Observatories Astrophysics Series*, Vol.4, Cambridge University Press
- Ojha, D. K. 2001, *MNRAS*, 322, 426
- Pohlen, M., Dettmar, R.-J., & Lütticke, R. 2000a, *A&A*, 357, L1
- Pohlen, M., Dettmar, R.-J., Lütticke, R. & Schwarzkopf, U. 2000b, *A&AS*, 144, 405
- Pohlen, M., 2001, *PhD Thesis*, Ruhr-University Bochum, Germany
- Pohlen, M., Dettmar, R.-J., Lütticke, R., & Aronica, G. 2002, *A&A*, 392, 807
- Pohlen, M., et al. 2004, in prep.
- Quinn, P. J., Hernquist, L., & Fullagar, D. P. 1993, *ApJ*, 403, 74
- Raha, N., Sellwood, J. A., James, R. A., & Kahn, F. D. 1991, *Nature*, 352, 411
- Sackett, P. D., Morrison, H. L., Harding, P., & Boroson, T. A. 1994, *Nature*, 370, 441
- Shaw, M. A. & Gilmore, G. 1989, *MNRAS*, 237, 903
- Shaw, M. A. & Gilmore, G. 1990, *MNRAS*, 242, 59
- Silva, D. R., Boroson, T. A., Thompson, I. B., & Jedrzejewski, R. I. 1989, *AJ*, 98, 131
- Spitzer, L. J. & Schwarzschild, M. 1953, *ApJ*, 118, 106
- Tsikoudi, V. 1979, *ApJ*, 234, 842
- Tsikoudi, V. 1979, *ApJS*, 43, 365
- van der Kruit P. C., 1979, *A&AS* 38, 15
- van der Kruit P. C., 1988, *A&A* 192, 117
- van der Kruit, P. C. & Freeman, K. C. 1986, *ApJ*, 303, 556
- van der Kruit, P. C. 1984, *A&A*, 140, 470
- van der Kruit P. C., Searle, L., 1981a, *A&A* 95, 105
- van der Kruit P. C., Searle, L., 1981b, *A&A* 95, 116
- van Dokkum, P. G., Peletier, R. F., de Grijs, R., & Balcells, M. 1994, *A&A*, 286, 415
- Velazquez, H. & White, S. D. M. 1999, *MNRAS*, 304, 254
- Wielen, R. 1977, *A&A*, 60, 263
- Wielen, R., Dettbarn, C., Fuchs, B., Jahreiß, H., & Radons, G. 1992, *IAU Symp.* 149: *The Stellar Populations of Galaxies*, 149, 81
- Wu, H., Burstein, D., Deng, Z. et al. 2002, *AJ*, 123, 1364
- Zheng, Z., Shang, Z., Su, H. et al. 1999, *AJ*, 117, 2757

## Appendix A: Comments on Individual Galaxies

**NGC 1596:** (Fig. B.1) A ‘normal’ S0 enclosed in a huge, spheroidal, outer envelope possibly triggered by interaction with the nearby physical companion (NGC 1602). The difference from other S0s is obvious from radial cuts. It is the only galaxy in which the profiles bend upwards (not caused by a background gradient) at larger galactocentric distances ( $R = \pm 115''$ ). This looks similar to an  $R^{1/4}$  bulge component beginning to dominate the profile when extrapolating the curvature of the inner bulge towards the outer extension. However, the overall flatness of such an  $R^{1/4}$  bulge would be unusual. In addition, the contours start to show substructure in the very outer parts (in contrast to the smooth contours of ellipticals). The inner light profiles are dominated by bulge and a possible inner disk component. The major axis shows several distinct parts: an inner bulge, a steep straight decline out to  $R \approx \pm 80''$ , an asymmetric slightly shallower part out to  $R = -110''$  and  $R = +120''$ , followed by an upwards bending profile an upbending profile. The SW-side is slightly more extended than the NE-side. After the outer thick disk has been subtracted, the remaining profiles clearly resemble still the thin/thick disk behaviour (changing of slopes towards outer/higher radial cuts), therefore no consistent model could be derived.

**NGC 2310:** (Fig. B.2) exhibits a box-shaped bulge (type 2 according to Lütticke et al., 2000a). The bulge/bar is rotated  $\approx 0.5^\circ$  against the outer disk, therefore we find

a slightly tilted residual. The radial profiles show a complex structure with inner, small, very bright nuclear bulge component, and further out a significant dip in the profile (caused by a possible dust ring or mimicked by a subsequent stellar ring), sitting on top of a bar/ring-like structure  $R \approx \pm 50''$ . There is a narrow disk-like structure  $R \approx \pm 82''$ , here assumed to be the main underlying disk, finally showing a straight decline into the noise (NE-side disturbed by nearby star-halo). The best fitting model overestimates the inner disk component due to inner ring-like feature. This feature is responsible for the apparent holes in the residual image, which shows the inner box-shaped bulge in addition to a large ring or bar.

**ESO 311-012:** (Fig. B.3) Box-shaped bulge (type 2 according to Lütticke et al., 2000a). The galaxy position is close to the Galactic plane with many foreground stars overimposed. The bulge component is still visible on the minor axis high above the plane. The radial profile shows a bar-like structure at  $R = \pm 20''$ , followed by an exponential disk component out to a break at  $R \approx \pm 83''$ . The residual is a box-shaped bulge with the indication of a weak bar extending on both sides.

**NGC 3564:** (Fig. B.4) The galaxy is probably part of small group/cluster with at least two large, nearby physical companions (NGC 3568 and NGC 3557). Taking into account the low surface brightness part it is different from the other S0s. Out to  $\mu_V = 23.4 \text{ mag}/\square''$  it looks similar although with a more dominating bulge. The outer contours, on the other hand, reveal that NGC 3564 is sitting in a huge, roughly spherical stellar envelope, which has probably been built up by a merger with a smaller satellite galaxy still visible in this structure on the NE-side ( $(R, z) = -47'', +24''$ , distance unknown). The radial profile shows an inner bulge-dominated part, followed by a bar-like plateau  $R \approx \pm 10''$ , sitting on top of an inner disk structure out to  $R \approx \pm 30''$  which is followed by a straight decline into noise. The residual resembles a rather large, spheroidal inner bulge together with a bar or ring-like structure extending to both sides. It nicely shows the possibly merging satellite. The thick disk component takes most of the light from the envelope and therefore the remaining bulge light is comparable to that of the other galaxies.

**NGC 3957:** (Fig. B.5) Galaxy cluster in background. Nearly box-shaped bulge (type 3 according to Lütticke et al., 2000a). It is an S0 galaxy with unusual, inner ( $R \lesssim \pm 30''$ ) dust lane. The bulge component is still visible on the minor axis high above the plane. The radial profiles show inner bulge, followed by a ring- or bar-like component at  $R \approx \pm 30''$  (visible in cuts above the dust lane), with break at  $R \approx \pm 60''$  and followed by a straight decline into the noise. The profile probably starts to bend outwards from  $R \approx \pm 105''$  ( $\mu_V \gtrsim 24.3 \text{ mag}/\square''$ ) to  $R \approx \pm 150''$ . The residual resembles a nearly box-shaped bulge with an indication of a bar extending to both sides. The apparent holes are caused by absorption in the inner dust lane.

**NGC 4179:** (Fig. B.6) The inner bar/bulge component is rotated  $\approx 0.5^\circ$  against the outer disk. The major axis shows a bright inner bulge, a disk- or bar-like feature between  $R \approx \pm 40''$  ( $z \lesssim \pm 5''$ ), a more shoulder-like decline out to  $R \approx \pm 80''$ , here taken to be the main underlying disk, followed by a straight decline into the noise. The residual resembles a spheroidal bulge with an indication of an inner disk or bar extending slightly to both sides.

**NGC 4521:** (Fig. B.7) The inner component is  $\approx 1^\circ$  rotated against the outer disk. The radial profile shows a bar- or ring-like structure between  $R \approx \pm 20''$  out to  $z \lesssim \pm 5''$ ; on top of a two-slope disk, inner part out to a break radius of  $R \approx -60''$ , followed by a steeper straight decline out to  $R \approx -77''$  and a slightly upwards bending part at the very edge (perhaps flatfield problem). The only galaxy with inconsistent thick/thin disk fitting without obvious reason (cf. NGC 1596). All trials, such as changing vertical fitting function, have failed. When various thick disk models have been subtracted, the resulting thin disks always contributes too much light in the outer/higher  $z$  profiles dominated by the thick disk. Because of this the following thick disk is flattened, producing an unstable situation, perhaps caused due to lower image quality, proximity to chip edge, and disturbed by bright star on the NW-side. In principle, the galaxy exhibits the same features in radial/vertical cuts as our other S0s.

**NGC 5047:** (Fig. B.8) Peanut-shaped bulge (type 1 according to Lütticke et al., 2000a). There are many companions around associated with the foreground NGC 5044 group of galaxies ( $\Delta v \approx 3600 \text{ km s}^{-1}$ ). Outer disk has a slightly s-shaped warp, on the SW-side towards N, on the NE-side towards S. The inner disk part is slightly off-centered to the outer component. The radial profiles show a bar-, or ring-like feature between  $R \approx \pm 30''$  out to  $z \lesssim \pm 3''$ , on top of a shoulder-like inner disk out to  $R \approx \pm 50''$ , followed by a straight decline out to  $\mu_V \gtrsim 25.0 \text{ mag}/\square''$ . The residual shows a nice peanut-shaped bulge with a thin bar-like component. The ratio of the bar length to the maximum of the peanut distortion closely matches simulations explaining the peanut by dynamical processes in the bar potential (cf. Lütticke et al., 2000b).

## Appendix B: Isophote maps, radial/vertical profiles, and residual images

The following figures show in the *upper panel* an isophote map of each galaxy rotated to the major-axis. A small arrow in the upper right corner indicates the North. The magnitude of the outer contour ( $\mu_{\text{lim}}$ , defined by a  $3\sigma$  criterion of the background) is indicated in each plot. The consecutive contours are equally spaced by  $0.5 \text{ mag}$ . The contour lines are plotted with increasing smoothing towards the outer parts. For the inner contours out to where the noise begins to increase no smoothing was applied. The following 2-3 contours are smoothed by replacing each pixel by the mean of  $3^2$ -pixels "around" the central pixel. For the outer two contours this smoothing is increased to  $5^2$ -pixels. The *second panel* displays the major-axis sur-

face brightness profile (top) and two parallel radial profiles each above and below the major axis. The exact  $z$ -positions for the plotted profiles are indicated in the upper left corner of the plot. For a consistent thin/thick disk decomposition the model profiles are overplotted as dashed lines. The *third panel* displays the minor-axis surface brightness profile (top) and two parallel vertical profiles on either side of the minor-axis. Again the exact  $R$ -positions for each cut are marked in the upper left corner and the best model is overplotted with dashed lines. The *lower panel* is the isophote map of the residual image after subtracting the best fitting thin/thick disk model. The magnitude of the outer contour ( $\mu_{\text{lim}}$ ) is again indicated in each plot and the following contours are equally spaced by 0.5 mag.

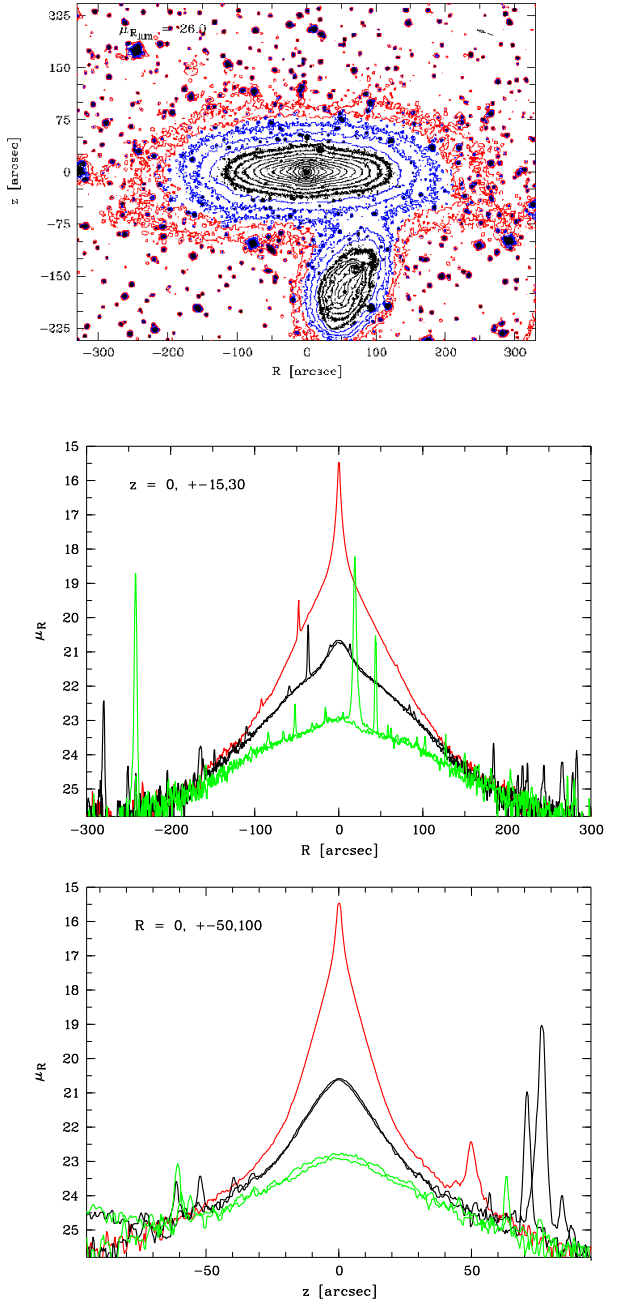


Fig. B.1. NGC 1596 R-band

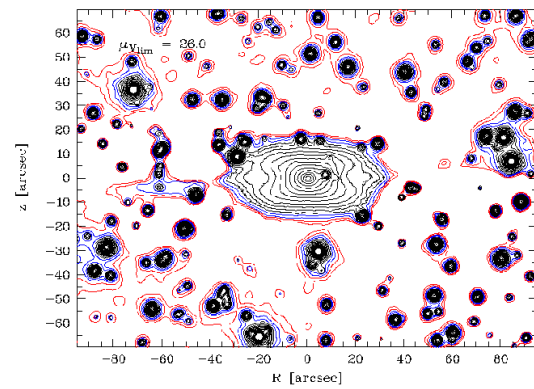
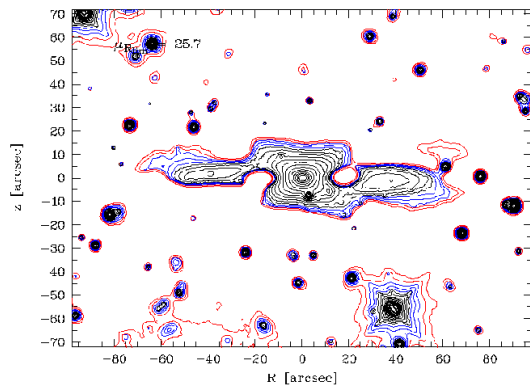
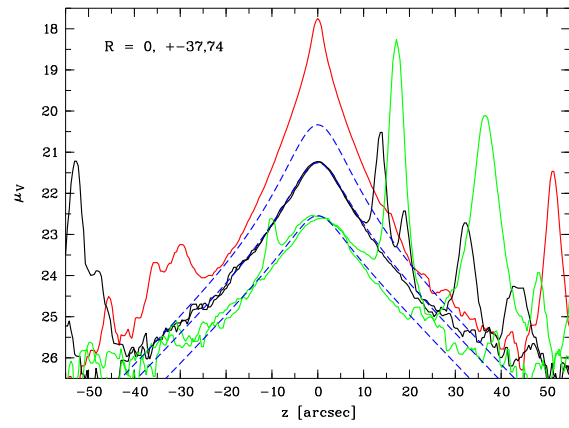
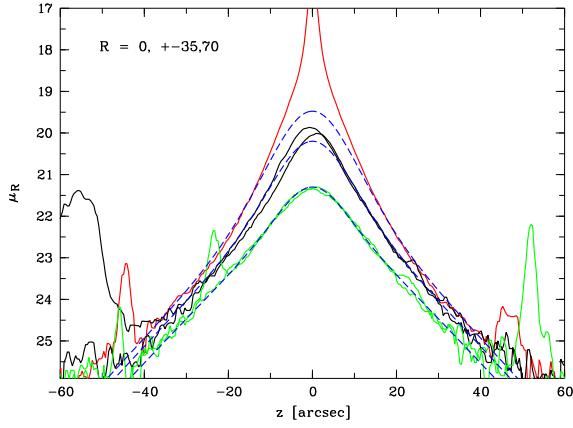
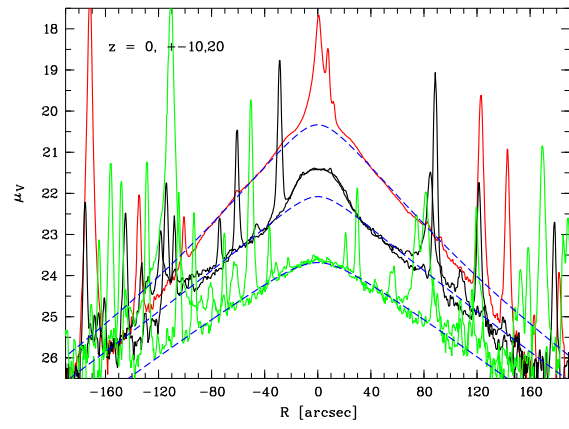
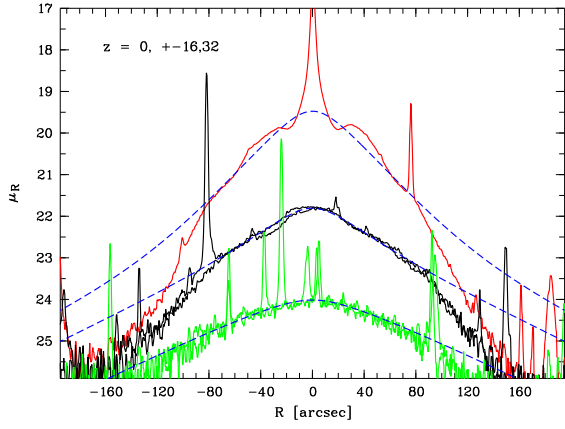
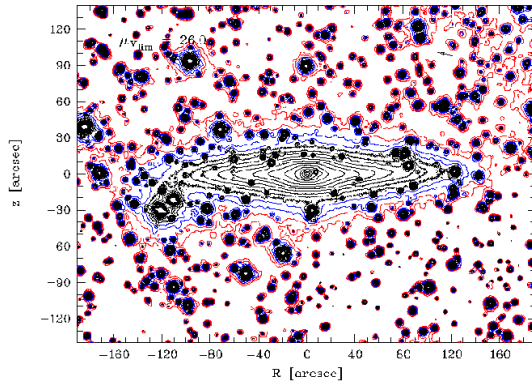
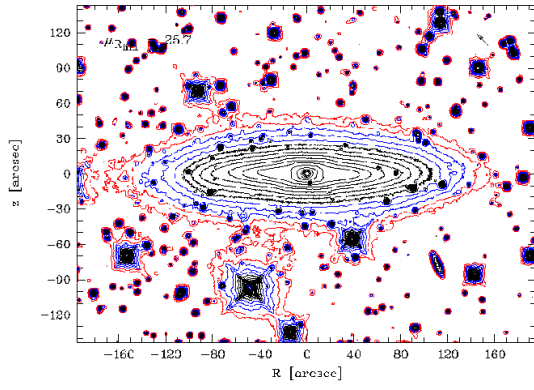


Fig. B.2. NGC 2310 R-band

Fig. B.3. ESO 311-012 V-band

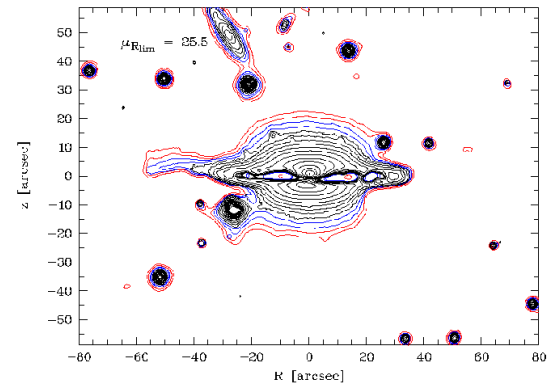
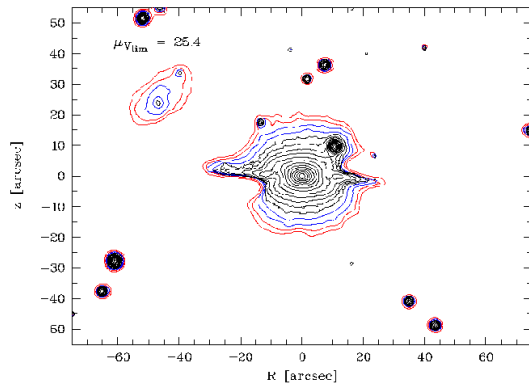
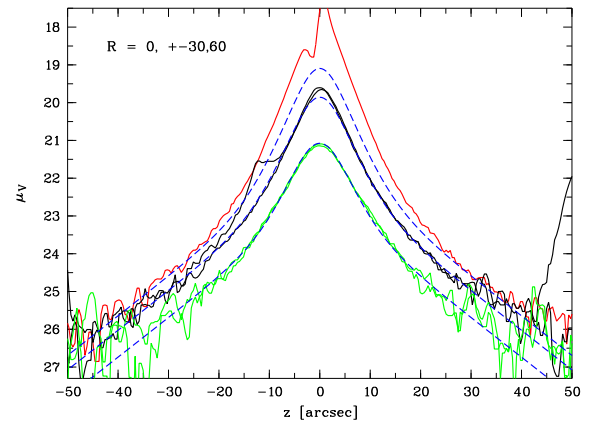
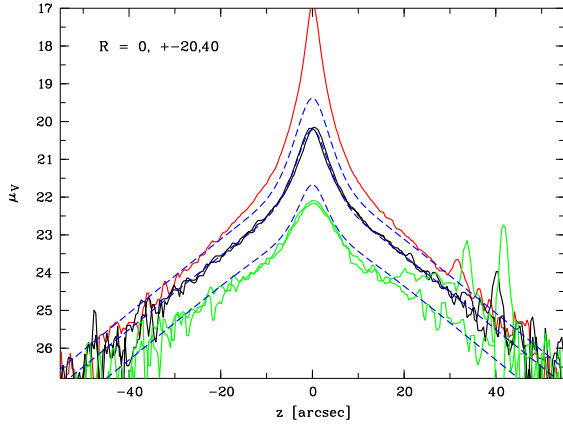
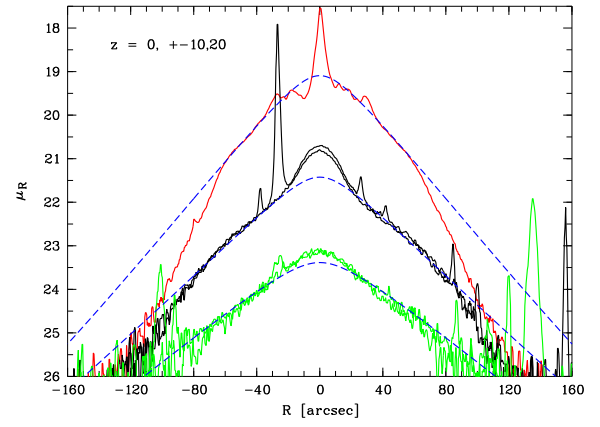
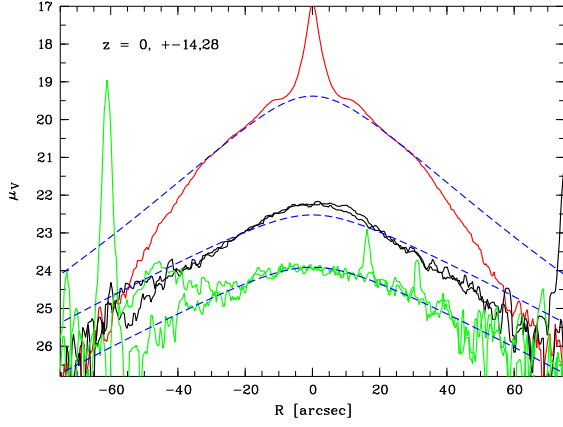
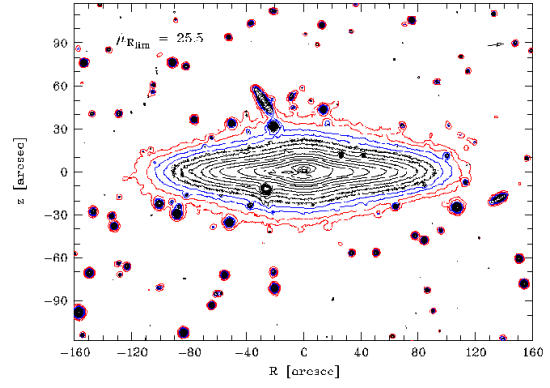
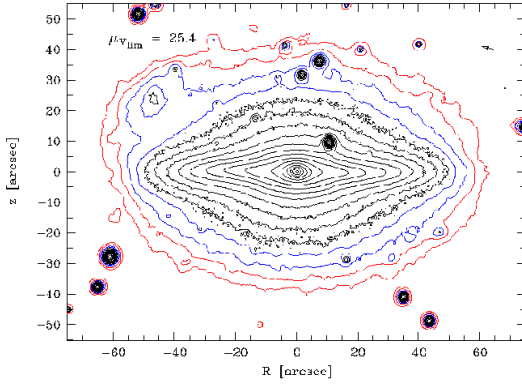


Fig. B.4. NGC 3564 V-band

Fig. B.5. NGC 3957 V-band



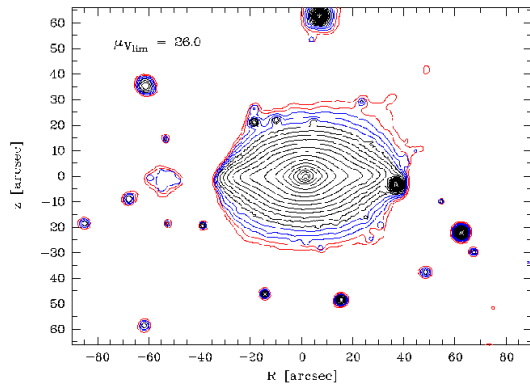
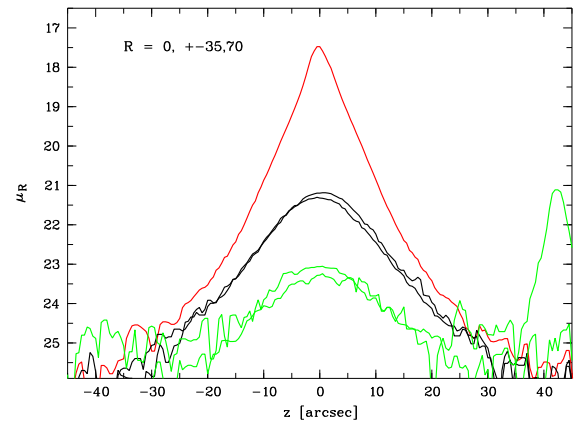
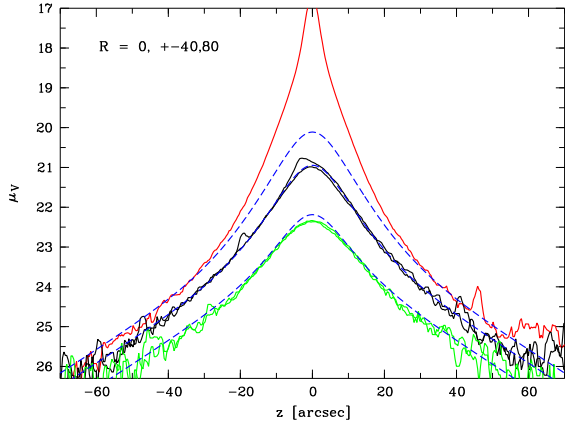
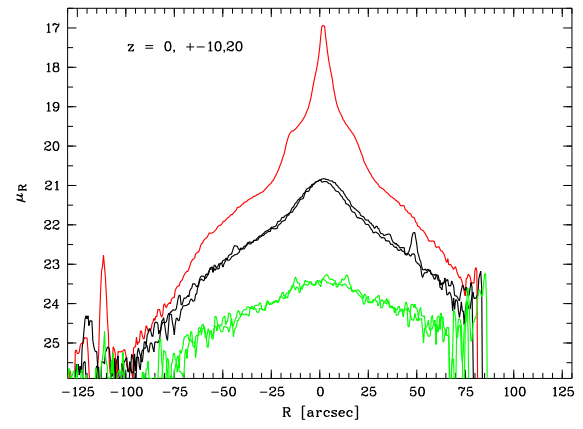
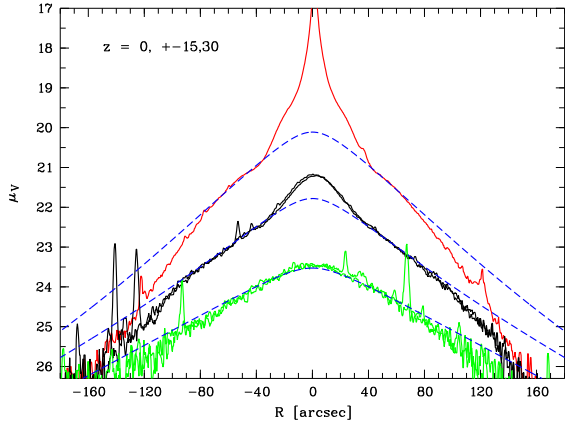
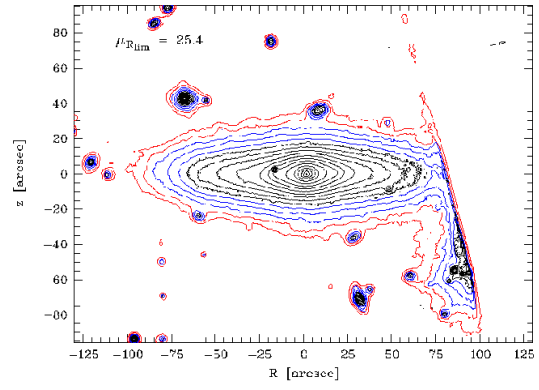
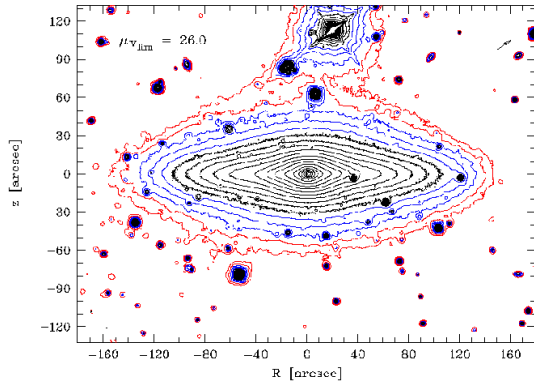


Fig. B.6. NGC 4179 V-band

Fig. B.7. NGC 4521 R-band



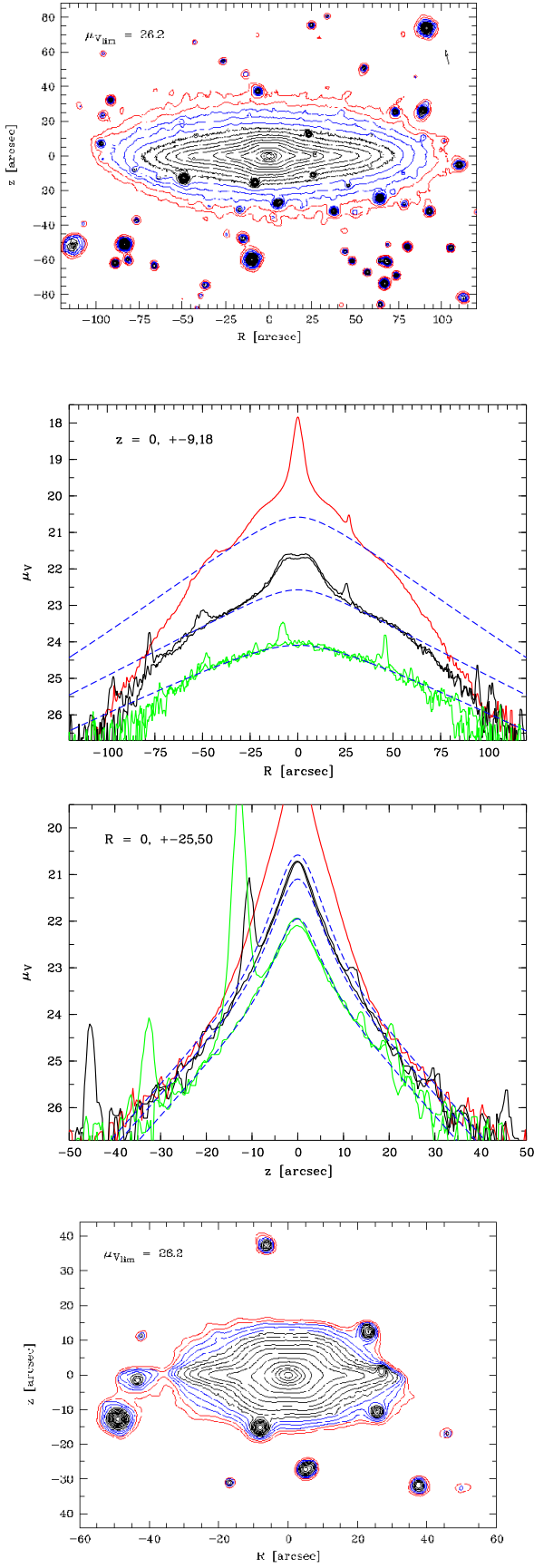


Fig. B.8. NGC 5047 V-band